Deep-Sea Research I 88 (2014) 1–7

Contents lists available at ScienceDirect

Deep-Sea Research I

journal homepage: www.elsevier.com/locate/dsri

Note

Decadal change of Antarctic Intermediate Water in the region of Brazil and Malvinas confluence

Xiao-Yi Yang [a,b,*], Zhigang He [b]

[a] State Key Laboratory of Marine Environmental Science, Xiamen University, Xiang an Campus, 361102 Xiamen, Fujian, China
[b] College of Oceanography and Earth Sciences, Xiamen University, Xiang an Campus, 361102 Xiamen, Fujian, China

ARTICLE INFO

Article history:
Received 18 July 2013
Received in revised form
25 February 2014
Accepted 27 February 2014
Available online 7 March 2014

Keywords:
Antarctic Intermediate Water (AAIW)
Brazil and Malvinas current confluence
Decadal change
Eddy buoyancy flux
Potential vorticity (PV)

ABSTRACT

The Antarctic Intermediate Water (AAIW) exhibits a decadal variability during recent years, i.e., salinification before 1997 and freshening thereafter, with the maximum anomalies locating at the region of Brazil and Malvinas currents confluence. Our study proposed that the local mesoscale eddies may play an important role in triggering this decadal oscillation. The eddy activity intensification (weakening) leads to the increase (decrease) of poleward cross-frontal eddy salinity flux and upward eddy buoyancy flux, which results in the weakening (strengthening) of the subsurface stratification and potential vorticity (PV). The PV anomalies facilitate (block) the poleward transport of warm saline subtropical water, while the stratification weakening favors the further downward transmission of salinity anomalies by processes of eddy flux as well as mean-flow advection (the stratification strengthening inhibits the vertical transport), then initiates the decadal change of the AAIW property. The whole process of the eddy-related propagation of salinity anomalies takes about 4 to 6 years.

1. Introduction

The AAIW has universally been regarded as one of the most important water masses in the world oceans. Originated in the high-latitudes of Southern Hemisphere (SH), AAIW spreads northward all the way to three ocean basins, and exchanges the heat, freshwater and carbon dioxide between them. Particularly in the Atlantic ocean, it can be traced across the equator and extend as far north as 30°N (Talley, 1996).

The controversy about AAIW were never settled down, involving first its origin and then its water mass property change. Some early studies agreed on the circumpolar formation of AAIW by along-isopycnal subduction of Antarctic Surface Water (AASW) (Deacon, 1937; Sverdrup et al., 1942). McCartney (1977) suggested the AAIW is mostly originated from Subantarctic Mode Water (SAMW) due to winter deep convection at the both ends of Drake Passage. Molinelli (1981), in recognizing the non-uniform renewal of AAIW, proposed that the isopycnal mixing of AASW across the Polar Front dominates the AAIW formation. The subsequent observational analyses and numerical simulations support either winter deep convection mechanism (England et al., 1993), or isopycnal processes across PF (Sørensen et al., 2001; Santoso and England, 2004), or their combination (e.g., Piola and Georgi, 1982; Piola and Gordon, 1989; Talley, 1996; Sloyan and Rintoul, 2001; Saenko et al., 2003).

The aggregation of the high-quality repeat hydrographic sections makes it possible to detect the long-term change of AAIW and SAMW property. Some studies reported the warming and/or freshening of the intermediate layers in the SH oceans, including South Pacific (Bindoff and Church, 1992; Johnson and Orsi, 1997; Shaffer et al., 2000), South Atlantic (Arbic and Owens, 2001), South Indian oceans (Wong et al., 1999; Bindoff and McDougall, 2000) and the Southern Ocean as a whole (Gille, 2002). The model simulations further revealed that the changes of AAIW/SAMW property can be mostly traced back to its outcrop region, where the Ekman transport, surface heat and fresh water fluxes vary in response to the anthropogenic forcing (Banks et al., 2000; Banks and Bindoff, 2003; Santoso and England, 2004; Fyfe, 2006). However, Bryden et al. (2003) compared five trans-Indian hydrographic sections ranging from 1936 to 2002 and proposed that SAMW property variability exhibits a decadal oscillation—freshened before 1987 and become saltier hereafter, rather than a linear trend of freshening. The work by Schneider et al. (2005) demonstrated that AAIW turned warmer and saltier in the eastern South Pacific between 1992 and 2003. In the subtropical South Atlantic, the AAIW presents a consistent warming trend since 1950s, but a significant salinification from 1950s to 1990s and a freshening

* Corresponding author at: Xiamen University, State Key Laboratory of Marine Environmental Science, C3-418, Xiping Building, Xiang an Campus, Xiamen 361102, Fujian, China. Tel.: +86 592 218 7671; mob.: +86 158 8027 2957.
E-mail address: xyyang@xmu.edu.cn (X.-Y. Yang).

http://dx.doi.org/10.1016/j.dsr.2014.02.007
0967-0637

after 1990s (McCarthy et al., 2011). The warming and lightening trends of AAIW property persisted into the 2000s, probably reflecting the air-sea turbulent heat flux and sea ice formation trends in its origin regions (Close et al., 2013). In contrast, there is no pronounced long-term AAIW salinity trend, despite a strong variability on decadal time scales (Schmidtko and Jonhson, 2012).

The previous AAIW property change studies are mostly based on the in-situ observations, which, though robust enough, lacks the continuity in both spatial and temporal dimensions. This probably results in the ambiguity involving the decadal variability of AAIW salinity and its mechanisms. Using an assimilated reanalysis dataset, this study proposes a prominent decadal variability of AAIW since 1990s and attributes it to the eddy activity in the southwestern Atlantic.

2. Data and method

The simple ocean data assimilation (SODA) reanalysis dataset is constructed by assimilating all available observational data, including hydrographic profiles, ocean station data, and infrared satellite data, to the Parallel Ocean Program (POP) ocean model output (Carton and Giese, 2008). Here the newly released SODA v2.2.4 is used with the resolution of $0.5^\circ \times 0.5^\circ \times 40$-level spatially and monthly mean ranging from Jan 1871 to Dec 2008 temporally. Compared with the previous versions, this version improves its surface forcing boundary conditions and assimilates more recent observation data, wherefore does a better job on bias suppression (Giese et al., 2011; Giese and Ray, 2011).

To verify the reanalysis data results, the high-resolution conductivity–temperature–depth (CTD) data and profiling float (PFL) data from the World Ocean Database 2009 (WOD09) and the weekly sea surface height anomaly data from AVISO TOPEX/Jason 1 merged satellite product are used in this study. In addition, the other two products of ocean reanalysis data (including NCEP Global Ocean Data Assimilation System (NCEP-GODAS) and the ECMWF system 3 ocean analysis system (ECMWF-ORAs3)) and the GFDL coupled model simulation data are compared with the SODA data results. The NCEP-GODAS data is based on a quasi-global configuration of the GFDL MOMv3, with the resolution of $1^\circ \times 1^\circ$ enhanced to $1/3^\circ$ in the N–S direction within 10° of the equator and vertical 40 levels. GODAS assimilates temperature profiles from XBTs, TAO, TRITON, PIRATA moorings and Argo profiling floats (Behringer et al., 1998). The ECMWF ORAs3 is based on the Hamburg Ocean Primitive Equations (HOPE) ocean model, with the resolution of $1^\circ \times 1^\circ$ and 29 levels in the vertical. In addition to surface and subsurface temperature, this dataset also assimilates altimeter derived sea-level anomalies and salinity data (Balmaseda et al., 2007).

For all the monthly datasets, the high frequency variability is filter out by taking the 13-point running mean, as we focus on the decadal time scale. In addition, for a region with sharply changing isopycnal slope, we interpolate the grid data onto the dynamic height coordinate. The dynamic height is measured in dynamic meters and is defined by

$$D(p_1, p_2) = \int_{p_1}^{p_2} \delta(T, S, p) dp,$$

where p_1 and p_2 are two reference pressure levels, and δ the specific volume anomaly. Dynamic heights are preferred over meridional coordinate because the energy will be conserved along the dynamic height coordinate. Moreover, the dynamic height contours coincide with the geostrophic streamlines, hence the property averaged along the dynamic height coordinate approximates the calculation of a transport-weighted mean. (see Naveira Garabato et al., 2009; Close et al., 2013). The 500 dbar and 1500 dbar are chosen as the reference pressure levels in order to emphasize the dynamics in the intermediate levels.

3. Results

The AAIW is characterized by a salinity minimum layer, with a typical salinity of 34.2–34.4 psu and temperature of 3–5 °C. The density surfaces associated with the core of AAIW fall in the range 1027.1–1027.3 kg/m^3 (Molinelli, 1981; Piola and Georgi, 1982), which is well reproduced in the SODA climatological data (figure not shown). Following the earlier studies (e.g., Santoso and England, 2004), the θ-S properties in the SODA data are interpolated onto the typical potential density surface of AAIW ($\sigma_\theta = 27.2$), and the zonal-mean AAIW salinity variability is shown in Fig. 1a. The prominent change occurs at the time about mid-1990s, with nearly neutral state for the pre-1995 period but large positive anomalies followed by negative anomalies for the

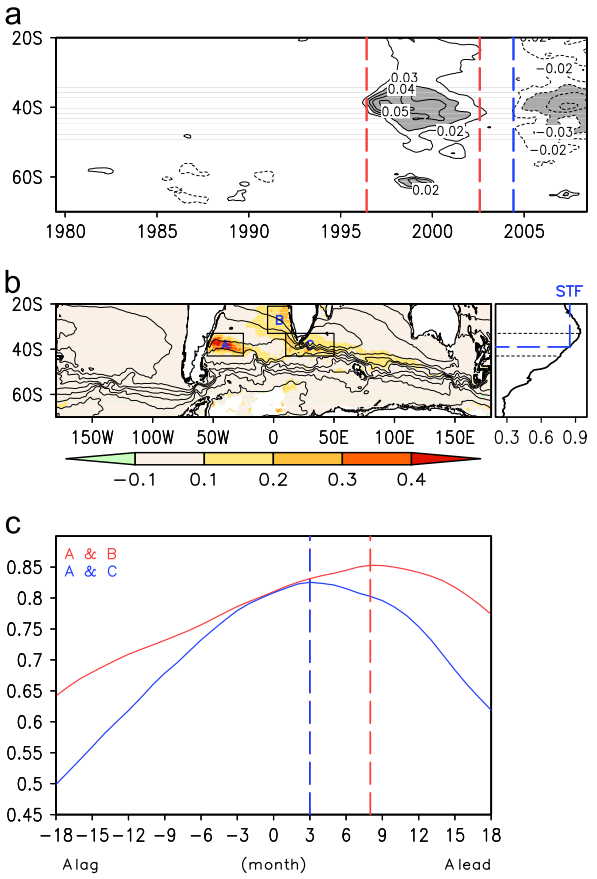

Fig. 1. (a) Zonal mean AAIW ($\sigma = 27.2$) salinity anomalies during 1979–2008 period in the SODA data, with the anomalies exceeding ± 0.03 psu shaded. Dashed lines denote the periods of high salinity (1996.6–2002.8, red) and low salinity (2004.6–2008.12, blue) periods; (b) AAIW salinity composite for high minus low salinity periods (defined by the dashed lines in Fig. 1a, shading) and the 1979.1–2008.12 climatology of 500–1500 dbar dynamic heights with the intervals of 0.3, 0.4, 0.5, 0.6, 0.7, 0.8, 0.9, 1.0 …… (contours, unit: dynamic meter). The rectangles indicate the BMC region (region A, 55–25°W, 43–33°S), the subtropical southeast Atlantic (region B, 5°W–15°E, 33–21°S) and the Agulhas return flow (region C, 10–50°E, 43–33°S), respectively. The BMC zonal-mean 500–1500 dbar dynamic heights are shown in the right panel, with the position of subtropical front indicated by blue dashed lines; (c) the lead-lag correlation coefficients of region A area-mean AAIW salinity with region B area-mean AAIW salinity (red), and of region A area-mean AAIW salinity with region C area-mean AAIW salinity (blue). The horizontal axis is the lead-lag months, with the negative values denoting region A lag region B (region C) by months. (For interpretation of the references to color in this figure legend, the reader is referred to the web version of this article.)

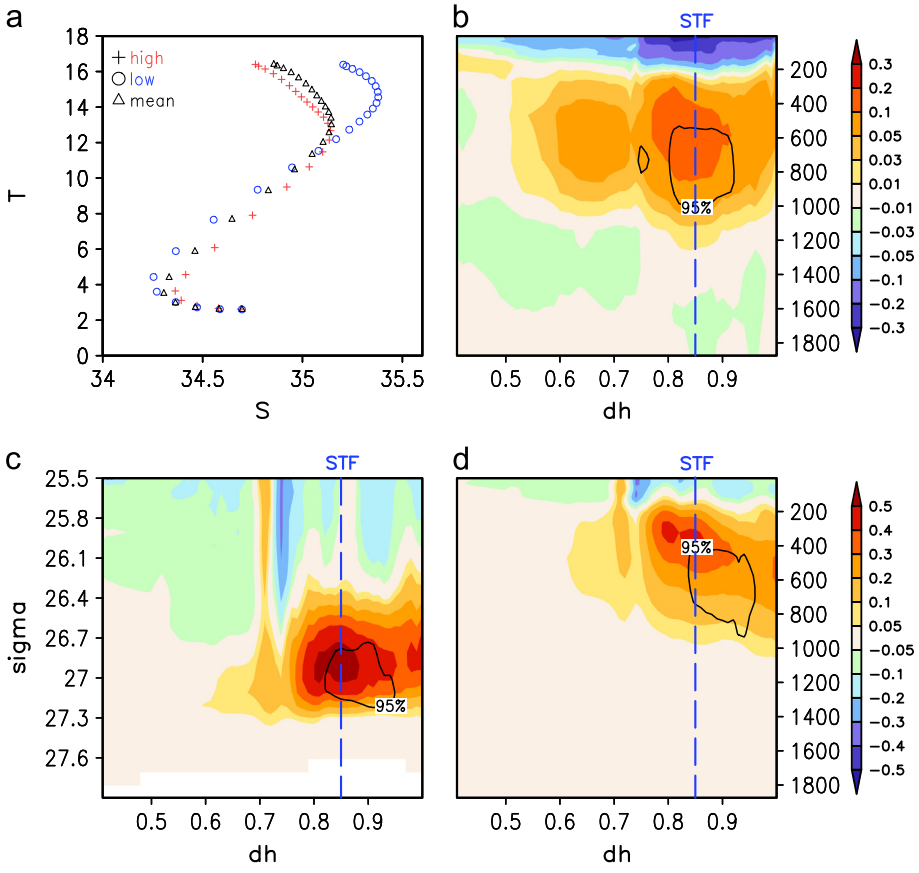

Fig. 2. (a) The BMC (region A) area-mean T-S diagram of 1979–2008 climatology (black triangle), composites for high (red cross) and low (blue circle) AAIW salinity periods from surface to intermediate layer (1875 m). (b) The BMC along-stream mean potential density composites (AAIW S high minus low) in the dynamic height-pressure coordinates (shading). The black contours indicate the 95% significance level of *t*-test, and the subtropical front position is marked by dashed blue line. (c) Same as (b), but for the salinity composites in the dynamic height-neutral density coordinates. (d) Same as (b), but for the salinity composites in the dynamic height-pressure coordinates. (For interpretation of the references to color in this figure legend, the reader is referred to the web version of this article.)

post-1995 period. The maximum/minimum salinity change (exceeding ± 0.05 psu) centers in the midlatitude of about 40°S. This decadal change of salinity is associated with the decadal change of potential temperature and depth of isopycnal surfaces, i.e., the freshening corresponding to cooling and deepening of the AAIW, and vice versa (figures not shown). The spatial pattern of high (1996–2002) minus low (2004–2008) AAIW salinity composite (Fig. 1b) shows that the significant AAIW salinity change is mostly confined in the western South Atlantic (region A, 55–25°W, 43–33°S), where a confluence of the warm saline Brazil current and cold fresh Malvinas current (hereafter BMC) results in the sharp dynamic height gradient and thermohaline subtropical front (STF) at approximately 39°S (Garzoli and Giulivi, 1994; Jullion et al., 2010). The second maximal changes of AAIW salinity locate in the subtropical southeast Atlantic (region B, 5°W-15°E, 33–21°S) and the Agulhas return flow (region C, 10–50°E, 43–33°S), where the warm saline Indian ocean water mixes with the Atlantic water. The month-to-month lead-lag correlation analysis reveals that the AAIW salinity variability in the region A lead those in the region B (region C) by about 8 months (3 months) (Fig. 1c), with the correlation coefficients exceeding 0.8. This clearly manifests the BMC as a key region for the decadal variability of AAIW property, and the anomalies here can be advected downstream to the Indian Ocean and the subtropical south Atlantic along the Antarctic circumpolar current and the subtropical gyre.

Many studies reported that the AAIW freshening is always associated with the AAIW warming and lightening. In the BMC region, however, the decadal change of AAIW property is characterized by the simultaneous freshening (salinification), cooling (warming) and deepening (shoaling) in the 27.2 density surface. This result is further demonstrated in Fig. 2. The BMC area-mean T–S diagram in the pressure levels (Fig. 2a) shows that the freshening (salinification) of intermediate water (including AAIW and SAMW) corresponds to the salinification (freshening) of the surface water, with insignificant change in the temperature fields. This asymmetry of AAIW T-S variability may result in the displacement of density surface. To further investigate the AAIW variability dynamically, the BMC along-stream mean density and salinity composites on the dynamic height-pressure (neutral density) coordinate are shown in Fig. 2b–d, respectively. Obviously, the BMC water density between 600 and 1000 dbar exhibits a significant increase in association with the AAIW salinification, indicating the shoaling of the intermediate density surface. This decadal variability of water density is consistent with the salinity change (Fig. 2d), with a remarkable salinification of the intermediate layer versus a slight freshening of the surface water. Given the drastic change of isopycnal surfaces across the BMC, the salinity anomalies are interpolated onto the neutral density surface. AAIW salinity anomalies on the isopycnal surfaces (Fig. 2c) are even greater than those on the pressure surfaces. The BMC water temperature, on the other hand, shows no decadal change on the pressure surface but significant warming (cooling) on the isopycnal surfaces during the period of 1996–2002 (2004–2008) (figures not shown). The fact that the salinity and temperature

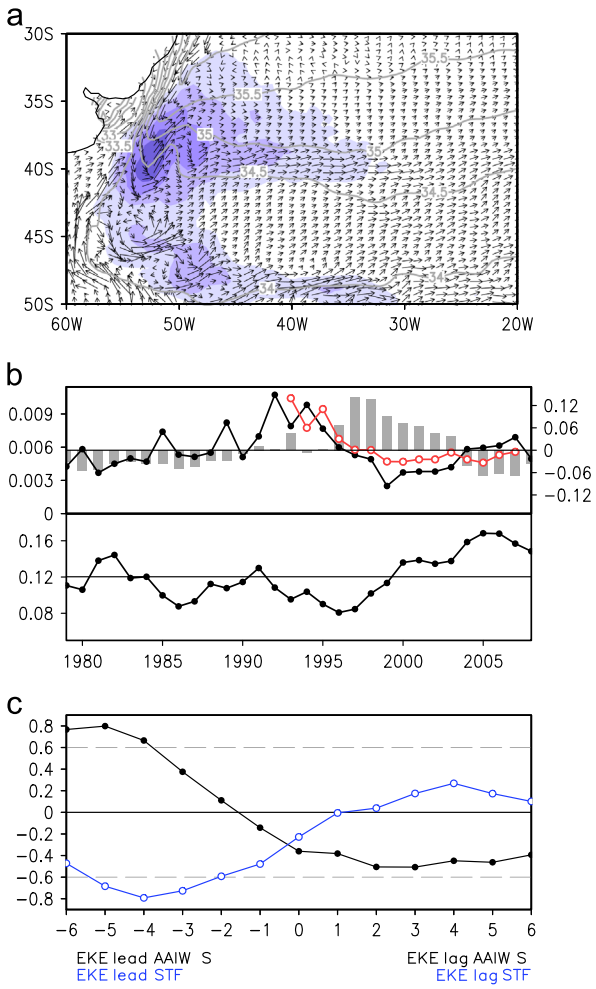

Fig. 3. (a) The BMC climatology of surface salinity (gray lines), horizontal velocity (vectors) and eddy kinetic energy (EKE, shades); (b) time series of BMC annual surface EKE (unit: m^2/s^2) from SODA dataset (SEKEI, black line) and from TOPEX satellite observations (red line), and a time series of AAIW salinity anomalies (gray bars) (upper panel), and the time series of subtropical front (STF) intensity according to Orsi et al. (1995) (lower panel); (c) lead-lag correlations between SEKEI and AAIW salinity anomalies (black), and between SEKEI and STF intensity anomalies (blue). (For interpretation of the references to color in this figure legend, the reader is referred to the web version of this article.)

anomalies are larger along isopycnal than along pressure surfaces implies that the undulation of isopycnal surfaces may play an active role in the AAIW decadal change.

An intuitive question is why the AAIW anomalies appear primarily in the southwestern Atlantic domain and what process dominates its decadal change. Due to the sharp contrasts in θ-S property of the subantarctic and subtropical waters, the BMC is characterized by a complex thermohaline structure and three fronts from south to north, i.e., the subantarctic front (SAF), the STF, and the Brazil current front (BCF) (Jullion et al., 2010). Among others, the STF is generally regarded as the transition between the subtropical water and subantarctic water (Orsi et al., 1995) and thus associated with the most vigorous eddy fields by the baroclinic instability processes (Fig. 3a) (Olson et al., 1988; Willson and Rees, 2000; Saraceno et al., 2004; Jullion et al., 2010). Jullion et al. (2010) further suggest that the BMC hosted intense eddy-driven heat and salt fluxes in the SAMW/AAIW layers. The presence of an intense eddy activity is believed to be the main driver of water mass modifications and exchanges of heat and freshwater between the subtropical and subantarctic waters (Boebel et al., 1999; Sun and Watts, 2002), though the mechanisms involved remain unclear. The time series of BMC annual surface EKE, AAIW salinity and the STF intensity anomalies are plotted in Fig. 3b. Following Orsi et al. (1995), the STF intensity anomalies are calculated from the maximum meridional salinity gradient at the 100 m depth level of BMC region in unit of psu. The overall value of STF intensity (0.12 psu) is much lower than the typical STF intensity (~0.5 psu, see Orsi et al., 1995), probably due to the coarse resolution of the reanalysis data used in this study. Nevertheless, the reanalysis data is quantitatively consistent with satellite data in EKE field. After 1990s, all the time series present a significant decadal variability but in different phases. The lead-lag correlation analysis reveals that the intensification (weakening) of eddy activity leads both the salinification (freshening) of AAIW by 4–6 years and the weakening (strengthening) of STF by 2–5 years (Fig. 3c). In contrast, the STF position exhibits neither strong decadal change nor significant correlation with EKE (figure not shown).

To explore the connection between the eddy activity and the AAIW property, the eddy buoyancy fluxes ($\overline{v'b'}$, $\overline{w'b'}$) and potential density are regressed onto the BMC surface EKE index (hereafter SEKEI). The intensification of surface eddy activity leads to the prevailing upward eddy buoyancy flux in the BMC, which results in the significant positive (negative) anomalies of potential density in the subsurface (surface) layer (Fig. 4a and b). The increase of potential density corresponds to the isopycnal elevation, hence the stratification weakening in the subtropical intermediate layer (600–1000 dbar). The potential vorticity (PV) decreases in response to the stratification weakening, which, according to the PV conservation law, facilitates the poleward penetration of the subtropical water mass along the PV isolines (Fig. 4c and d). The lead-lag correlation analysis further demonstrates that the subsurface potential density (Fig. 4e) and intermediate PV (Fig. 4f) both exhibit the significant correlation with SEKEI, and the anomalies propagate poleward from subtropical (EKE lead 0–1 year) to BMC region (EKE lead 3–4 years). On the other hand, the intensification of eddy activity is associated with the poleward cross-frontal eddy salinity flux, thus the transmission of positive salinity anomalies from the subtropics to BMC subsurface ocean (Fig. 5a and b). Once the stratification weakened by lagging SEKEI of 3–4 years, both the eddy salinity fluxes (Fig. 5b) and the mean-flow salinity advection (Fig. 5c) favor to relay the positive salinity anomalies downward to intermediate layer, leading to the salinification of AAIW (Fig. 5d). The reverse process occurs for the weakening of eddy activity.

4. Conclusions and discussions

Our analyses reveal that AAIW in the southwestern Atlantic have been undergone a prominent decadal variability—salinification/warming during the pre-1997 period and freshening/cooling during the post-1997 period. Previous studies based on in-situ observations suggest that the AAIW salinity change in the subtropical south Atlantic is linked to either the Agulhas leakage from the Indian Ocean or the hydrological cycle in its source region (Schmidtko and Jonhson, 2012; McCarthy et al., 2011). In this study, we proposed that the AAIW change in the BMC region in the decadal time scale is also connected to the change of local eddy activity about 4 to 6 years ago. One feasible dynamical process can be described as: the strengthening of eddy activity is associated with the anomalous upward eddy buoyancy flux in the subtropical Atlantic subsurface, leading to the isopycnal elevation and hence weakening of stratification and PV in the intermediate water. The PV conservation law favors the cross-stream poleward invasion of subtropical water through BMC intermediate ocean. On the other hand, the poleward eddy salinity flux conducts the southward penetration of saline subtropical water. The salinity anomalies are

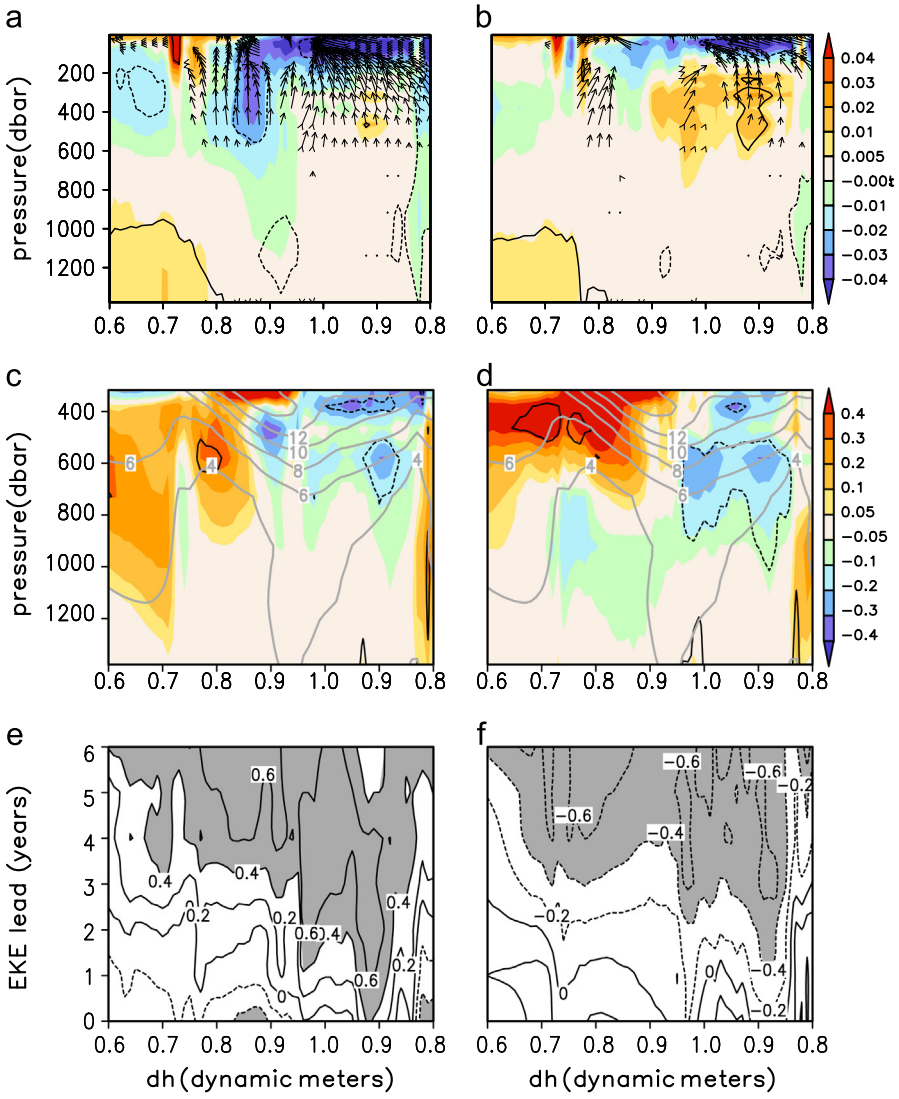

Fig. 4. (a) Dynamic height–pressure section of the regression coefficients of the BMC region along-stream (55–25°W mean) potential density (shades, with contours denoting the 95% significance level) and eddy buoyancy flux (vectors, only those vectors above 95% significance level are shown) on SEKEI; (b) same as (a), but for SEKEI leading potential density and eddy buoyancy flux by one year; (c) same as (a), but for SEKEI leading PV by one year, superposing the climatology of potential vorticity (gray contours). The PVs are multiplied by −1 to offset the effect of negative coriolis parameter f on PV values; (d) same as (c), but for SEKEI leading potential vorticity by two years; (e) correlation coefficients between SEKEI and subsurface (465 m) potential density with SEKEI leading by 0 to 6 years (the correlation coefficients above 0.4 are shaded); (d) same as (e), but for SEKEI and PV in intermediate layer (918 m).

further relayed downward by the eddy flux and mean-flow advection of salinity, resulting in the AAIW property change by lagging the SEKEI of 4–6 years.

It should be noted the south Atlantic are notoriously data sparse regions. Although the SOADv2.2.4 reanalysis assimilates all available in-situ data and improves its algorithm to suppress the systematic errors on decadal time scale (Giese et al., 2011), the data may be contaminated by certain spurious model results, especially for prior 1990s, when the satellite altimeter and WOCE data are not available. We compared the BMC area-mean AAIW salinity time series of the SODA data with the other two reanalysis products and a model simulation output (i.e., NCEP-GODAS, ECMWF-ORAs3 and GFDL model) (Fig. 6). Also plotted is the all available BMC region averaged CTD and PFL data from WOD09 database (gray bars). Three reanalysis datasets are generally consistent on the significant decadal change during the prior- and after-2004 periods, in spite of a large warm biases before 1990 in the NCEP-GODAS data. This warm biases are mostly due to a computational error in processing the XBT data for the year prior to 1990s. The correlation coefficient are as high as 0.75 for the SODA and ORAs3 data during 1979–2008, and 0.65 for the SODA and GODAS data during 1990–2008. Among all the datasets, the SODA data shows the highest correlation (~0.44) with the in-situ WOD09 data. In contrast, the pure model output without data assimilation processes like GFDL model output shows neither the signal of low-frequency variability nor correlation with the in-situ data. We should still be very cautious in evaluating the peak period of AAIW salinification (1997–2001) because no in-situ data is assimilated during this period. The maximum salinity anomalies in the SODA data are almost twice of those in the other datasets (Fig. 6). Moreover, the decadal change of AAIW salinity in the subtropical southeast Atlantic (region B) and the Agulhas return flow (region C) are also much larger than the in-situ data results of McCarthy et al. (2011) (see their Fig. 3 left panel) and Schmidtko and Jonhson (2012). Nevertheless, the AAIW decadal change since the late 1990s appears to be a robust feature regardless which reanalysis dataset is chosen. The fact that this decadal variability is closely connected to the eddy activity in the southwestern Atlantic should be underlined to improve the performance of general ocean circulation model.

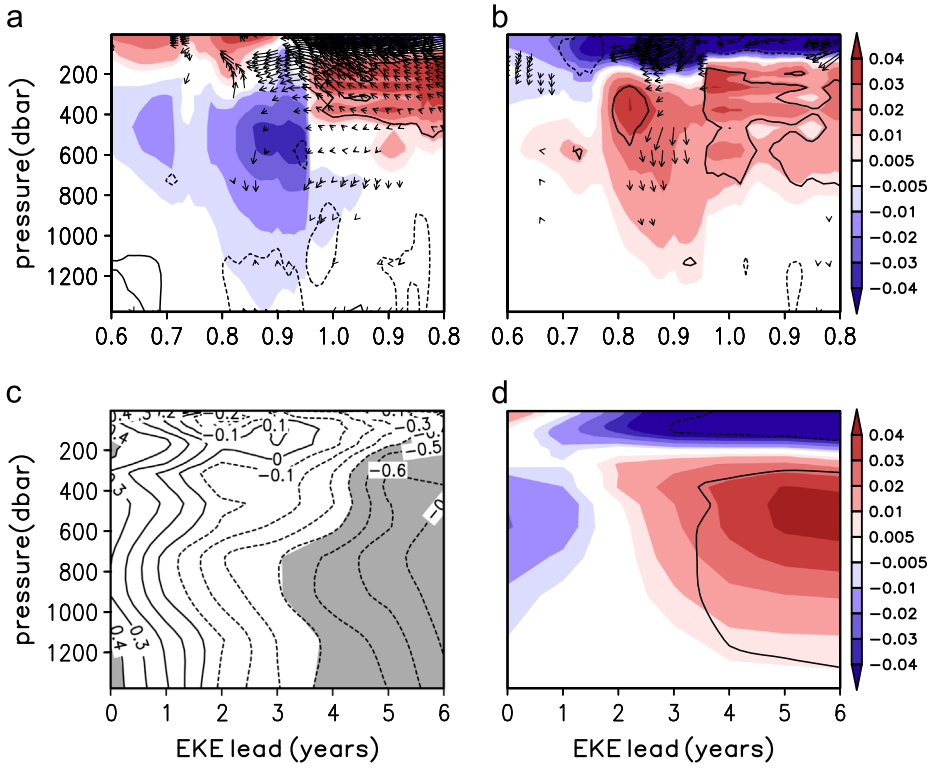

Fig. 5. (a) Same as Fig. 4a, but for SEKEI regression on the BMC region along-stream (55–25°W mean) salinity (shades) and eddy salinity flux (vectors); (b) same as (a), but for SEKEI leading by three years; (c) correlation coefficients between SEKEI and mean flow salinity transport (negative value means the downward transport) along 0.91 dynamic meter (SEKEI leading by 0–6 years); (d) same as (c), but for SEKEI regression on BMC area-mean salinity (shades, contours denoting 95% significance level).

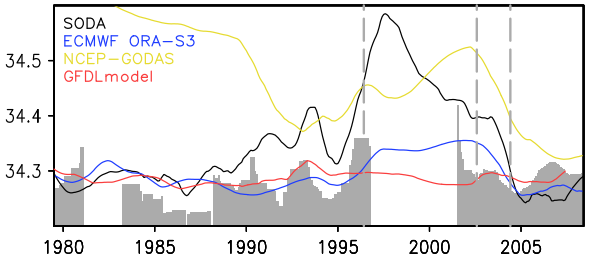

Fig. 6. Time series of the BMC area-mean AAIW (σ=27.2) salinity from the SODA (black), the ECMWF ORAs3 (blue), the NCEP-GODAS (yellow), the GFDL model (red), and the WOD09 in-situ (gray bars) datasets. (For interpretation of the references to color in this figure legend, the reader is referred to the web version of this article.)

Another important issue unresolved is the source of decadal change of AAIW and eddy activity in this region. McCarthy et al. (2011) attributed the decadal variability of Atlantic AAIW salinity to the inter-ocean exchange with Indian Ocean. Naveira Garabato et al. (2009), in contrast, proposed the joint influence of the El Nino-Southern Oscillation (ENSO) and the Southern Annular Mode (SAM) on the AAIW formation and property changes. Some studies reported the decadal change of the BMC upper ocean circulation after 1990s, such as the southward shift of the BCF, the confluence point of the Brazil and Malvinas currents, and the maximum wind stress curl (Goni et al., 2011; Lumpkin and Garzoli, 2011). This southward shift of the BCF may to some extent facilitate the cross-front mixing due to the closer proximity of the BCF and the STF. While the BMC happens to be one of the source region of AAIW, and the intense eddy activity in this region is influenced by many factors, like the surface wind stress, the subtropical front, and the oscillation of the confluence point, a freshwater budget diagnosis and numerical simulations are necessary for detecting the major mechanisms responsible for this AAIW decadal change in the future study.

Acknowledgments

Two anonymous reviewers are greatly appreciated for their insightful suggestions and comments. This study is supported by the National Basic Research Program of China (2012CB417402) and by the Natural Science Foundation of China (Grant 41006113).

References

Arbic, B.K., Owens, W.B., 2001. Climate warming of Atlantic Intermediate Waters. J. Clim. 14, 4091–4108.
Balmaseda, M., Vidard, A., Anderson, D., 2007. The ECMWF System 3 Ocean Analysis System. ECMWF Technical Memorandum, 508
Banks, H.T., Wood, R.A., Gregory, J.M., Johns, T.C., Jones, G.S., 2000. Are observed decadal changes in intermediate water masses a signature of anthropogenic climate change? Geophys. Res. Lett 27 (18), 2961–2964.
Banks, H.T., Bindoff, N.L., 2003. Comparison of observed temperature and salinity changes in the Indo-Pacific with results from the coupled climate model HadCM3: processes and mechanisms. J. Clim. 16, 156–166.
Behringer, D.W., Ji, M., Leetmaa, A., 1998. An improved coupled model for ENSO prediction and implications for ocean initialization. Part I: The ocean data assimilation system. Mon. Weather Rev 126, 1013–1021.
Bindoff, N.L., Church, J.A., 1992. Warming of the water column in the south-west Pacific. Nature 357, 59–62.
Bindoff, N.L., McDougall, T.J., 2000. Decadal changes along an Indian Ocean section at 32°S and their interpretation. J. Phys. Oceanogr. 30, 1207–1222.
Boebel, O., Schmid, C., Zenk, W., 1999. Kinematic elements of Antarctic Intermediate Water in the western South Atlantic. Deep Sea Res. 46, 355–392.
Bryden, H.L., McDonagh, E.L., King, B.A., 2003. Changes in ocean water mass properties: oscillations or trends? Science 300, 2086–2088.
Carton, J.A., Giese, B.S., 2008. A reanalysis of ocean climate using simple ocean data assimilation (SODA). Mon. Weather Rev. 136, 2999–3017, http://dx.doi.org/10.1175/2007MWR1978.1.
Close, S.E., Navera Garabato, A.C., McDonagh, E.L., King, B.A., Biuw, M., Boehme, L., 2013. Control of mode and intermediate water mass properties in Drake Passage by the Amundsen Sea Low. J. Clim. 26, 5102–5123.
Deacon, G.E.R., 1937. The Hydrology of the Southern Ocean, vol. 15. Cambridge University Press, pp. 3–12.
England, M.H., Godfrey, J.C., Hirst, A.C., Tomczak, M., 1993. The mechanism for Antarctic Intermediate Water renewal in a World Ocean model. J. Phys. Oceanogr. 23, 1553–1560.

Fyfe, J.C., 2006. Southern Ocean warming due to human influence. Geophys. Res. Lett. 33, L19701, http://dx.doi.org/10.1029/2006GL027247.
Garzoli, S., Giulivi, C., 1994. What forces the variability of the southwestern Atlantic boundary currents? Deep Sea Res. 41, 1527–1550.
Giese, B.S., Chepurin, G.A., Carton, J.A., Boyer, T.P., Seidel, H.F., 2011. Impact of bathythermograph temperature bias models on an ocean reanalysis. J. Clim. 24, 84–93.
Giese, B.S., Ray, S., 2011. El Nino variability in simple ocean data assimilation (SODA), 1871–2008. J. Geophys. Res. 116, C02024, http://dx.doi.org/10.1029/2010JC006695.
Gille, S., 2002. Warming of the Southern Ocean since the 1950s. Science 295, 1275–1277.
Goni, G.J., Bringas, F., DiNezio, P.N., 2011. Observed low frequency variability of the Brazil current front. J. Geophys. Res. 116, C10037, http://dx.doi.org/10.1029/2011JC007198.
Johnson, G.C., Orsi, A.H., 1997. Southwest Pacific Ocean watermass changes between 1968/69 and 1990/91. J. Clim. 19, 306–316.
Jullion, L., Heywood, K.J., Garabato, A.N., Stevens, D.P., 2010. Circulation and water mass modification in the Brazil–Malvinas confluence. J. Phys. Oceanogr. 40, 845–864.
Lumpkin, R., Garzoli, S., 2011. Interannual to decadal changes in the western South Atlantic's surface circulation. J. Geophys. Res. 116, C01014, http://dx.doi.org/10.1029/ 2010JC006285.
McCarthy, G., Mcdonagh, E., King, B., 2011. Decadal variability of thermocline and intermediate waters at 24°S in the South Atlantic. J. Phys. Oceanogr. 41, 157–165.
McCartney, M.S., 1977. Subantarctic Mode Water. In: Angel, M.V. (Ed.), A Voyage of Discovery: George Deacon 70th Anniversary Volume (Suppl. To Deep-Sea Res.). Pergamon, pp. 103–119
Molinelli, E.J., 1981. The Antarctic influence on Antarctic Intermediate Water. J. Mar. Res. 39, 267–293.
Naveira Garabato, A.C., Jullion, L., Stephens, D.P., Heywood, K.J., King, B.A., 2009. Variability of Subantarctic Mode Water and Antarctic Intermediate Water in Drake Passage during the late-twentieth and early-twenty-first centuries. J. Clim. 13, 3661–3688.
Olson, D.B., Podestá, G.P., Evans, R.H., Brown, O.B., 1988. Temporal variations in the separation of the Brazil and Malvinas currents. Deep Sea Res. 35, 1972–1990.
Orsi, A.H., Withworth III, T., Nowlin Jr, W.D., 1995. On the meridional extent and fronts of the Antarctic current. Deep Sea Res 42 (5), 641–673.
Piola, A.R., Georgi, D.T., 1982. Circumpolar properties of Antarctic Intermediate Water and Subantarctic Mode Water. Deep Sea Res 29, 687–711.
Piola, A.R., Gordon, A.L., 1989. Intermediate water in the southwestern South Atlantic. Deep Sea Res 36, 1–16.
Saenko, O.A., Weaver, A.J., England, M.H., 2003. A region of enhanced northward Antarctic Intermediate Water transport in a coupled climate model. J. Phys. Oceanogr. 33, 1528–1535.
Santoso, A., England, M.H., 2004. Antarctic Intermediate Water circulation and variability in a coupled climate model. J. Phys. Oceanogr. 34, 2160–2179.
Saraceno, M., Provost, C., Piola, A.R., Bava, J., Gagliardini, A., 2004. Brazil Malvinas frontal system as seen from 9 years of Advanced Very High Resolution Radiometer data. J. Geophys. Res. 109, C05027, http://dx.doi.org/10.1029/2003JC002127.
Schmidtko, S., Jonhson, G.C., 2012. Multidecadal warming and shoaling of Antarctic Intermediate Water. J. Clim. 25, 207–221.
Schneider, W., Fukasawa, M., Uchida, H., Kawano, T., Kaneko, I., Fuenzalida, R., 2005. Observed property changes in eastern South Pacific Antarctic Intermediate Water. Geophys. Res. Lett. 32, L14602, http://dx.doi.org/10.1029/2005GL022801.
Shaffer, G., Leth, O., Ulloa, O., Bendtsen, J., Daneri, G., Dellarossa, V., Hormazabal, S., Sehlstedt, P.-I., 2000. Warming and circulation change in the eastern South Pacific Ocean. Geophys. Res. Lett. 27 (9), 1247–1250.
Sloyan, B.M., Rintoul, S.R., 2001. Circulation, renewal, and modification and Antarctic Mode and Intermediate Water. J. Phys. Oceanogr. 31, 1005–1030.
Sørensen, J.V.T., Ribbe, J., Shaffer, G., 2001. Antarctic Intermediate Water mass formation in ocean general circulation models. J. Phys. Oceanogr. 31, 3295–3311.
Sun, C., Watts, D.R., 2002. Heat flux carried by the Antarctic Circumpolar current mean flow. J. Geophys. Res. 107, 3119, http://dx.doi.org/10.1029/2001JC001187.
Sverdrup, H.U., Johnson, M.W., Fleming, R.H., 1942. The Oceans: Their Physics, Chemistry, and General Biology. Prentice Hall p. 1987
Talley, L.D., 1996. Antarctic Intermediate Water in the South Atlantic.. In: Wefer, G., et al. (Eds.), The South Atlantic: Present and Past Circulation. Springer-Verlag, New York, pp. 219–238
Willson, H.R., Rees, N.W., 2000. Classification of mesoscale features in the Brazil–Falkland current confluence zone. Prog. Oceanogr. 45, 415–426.
Wong, A.P.S., Bindoff, N.L., Church, J.A., 1999. Large-scale freshening of intermediate waters in the Pacific and Indian Oceans. Nature 400, 440–443.